ELSEVIER

Check for updates

Predicting Alzheimer's disease severity by means of TMS—EEG coregistration

Chiara Bagattini [a,*], Tuomas P. Mutanen [b,c], Claudia Fracassi [a], Rosa Manenti [d], Maria Cotelli [d], Risto J. Ilmoniemi [b], Carlo Miniussi [a,e], Marta Bortoletto [a]

[a] Cognitive Neuroscience Section, IRCCS Istituto Centro San Giovanni di Dio Fatebenefratelli, Brescia, Italy
[b] Department of Neuroscience and Biomedical Engineering, Aalto University, Espoo, Finland
[c] Centre for Cognitive Neuroimaging, University of Glasgow, Glasgow, UK
[d] Neuropsychology Unit, IRCCS Istituto Centro San Giovanni di Dio Fatebenefratelli, Brescia, Italy
[e] Center for Mind/Brain Sciences- CIMeC, University of Trento, Rovereto, Italy

ARTICLE INFO

ABSTRACT

Clinical manifestations of Alzheimer's disease (AD) are associated with a breakdown in large-scale communication, such that AD may be considered as a "disconnection syndrome." An established method to test effective connectivity is the combination of transcranial magnetic stimulation with electroencephalography (TMS—EEG) because the TMS-induced cortical response propagates to distant anatomically connected regions. To investigate whether prefrontal connectivity alterations may predict disease severity, we explored the relationship of dorsolateral prefrontal cortex connectivity (derived from TMS—EEG) with cognitive decline (measured with Mini Mental State Examination and a face—name association memory task) in 26 patients with AD. The amplitude of TMS—EEG evoked component P30, which was found to be generated in the right superior parietal cortex, predicted Mini Mental State Examination and face—name memory scores: higher P30 amplitudes predicted poorer cognitive and memory performances. The present results indicate that advancing disease severity might be associated with effective connectivity increase involving long-distance frontoparietal connections, which might represent a maladaptive pathogenic mechanism reflecting a damaged excitatory—inhibitory balance between anterior and posterior regions.

© 2019 Elsevier Inc. All rights reserved.

1. Introduction

Alzheimer's disease (AD) is a common progressive neurodegenerative disorder that disturbs several cognitive functions with the core difficulties involving episodic memory (Dubois et al., 2007). Converging neuroimaging and electrophysiological results have demonstrated that the clinical manifestations of AD are not associated only with regional gray matter dysfunction but also with a breakdown in the communication between brain regions because of compromised large-scale connections, leading scientists to consider AD as a "disconnection syndrome" (Delbeuck et al., 2003). Magnetic resonance imaging (MRI), positron emission tomography (PET), and electroencephalography (EEG) have primarily indicated alterations in frontoparietal connectivity, together with weakened interhemispheric interactions (Berendse et al., 2000; Grady et al., 2001; Horwitz et al., 1987; Rose et al., 2000).

Loss of connectivity is not an "all at once" phenomenon in a brain affected by AD (Delbeuck et al., 2003) but rather connectivity is altered at several stages that mirror changes in AD pathology. In the prodromal and early stages of AD, resting-state functional MRI (fMRI) studies have consistently found a weakened connectivity in posterior brain regions (Agosta et al., 2012; Brier et al., 2012; Greicius et al., 2004; Sorg et al., 2007; Wang et al., 2006, 2007; Zhang et al., 2010; Zhou et al., 2010) coupled with an increased anterior connectivity, either within the prefrontal regions or between prefrontal areas and other brain regions (Agosta et al., 2012; Filippi et al., 2013; Supekar et al., 2008; Wang et al., 2006, 2007; Zamboni et al., 2013; Zhou et al., 2010). Looking at the full spectrum of AD pathology, abnormalities first affect the medial temporal lobe, the posterior cingulate cortex, and the precuneus (Braak and Braak, 1991; Buckner, 2005; Buckner et al., 2008; Greicius et al., 2004; Sorg et al., 2007; Sperling et al., 2010; Zhou et al., 2010), then spread to posterior lateral cortical areas, and finally to frontal regions in overt AD (Braak and Braak, 1991; Zhang et al., 2010).

Therefore, prefrontal cortex represents a crucial target area to investigate how connectivity is altered at different stages of AD

severity once clinical signs are overt, as these regions are affected in a late stage of the disease (Braak and Braak, 1991).

However, only a few works have investigated how connectivity alterations further change over time once AD symptoms are manifested. Zhang et al. (Zhang et al., 2010) investigated resting-state functional connectivity alterations in patients with mild, moderate, and severe AD, revealing that connectivity in the posterior cingulate cortex decreases but prefrontal connectivity increases with the progression of the disease. A longitudinal resting-state fMRI study by Damoiseaux et al. (2012) showed that connectivity decreased in posterior and increased in anterior areas at the very mild stage of the disease. However, when considering long-term changes, connectivity was found to decrease in all regions. Moreover, the functional implication of prefrontal connectivity alterations is still unclear. Although several authors have suggested that the enhanced prefrontal connectivity reflects a compensatory effect (Agosta et al., 2012; Gour et al., 2014; Supekar et al., 2008; Wang et al., 2006, 2007; Zamboni et al., 2013), the basis of such a phenomenon has not been elucidated (Pievani et al., 2014, 2011). According to the "compensatory hypothesis," patients with AD recruit additional frontal regions to compensate for the impaired posterior connectivity and for the resulting loss of cognitive functioning. An alternative explanation put forward by Pievani et al. (Pievani et al., 2014, 2011) is that, on the contrary, connectivity enhancement might represent a pathogenic mechanism because of damaged excitatory–inhibitory balance between anterior and posterior brain regions.

The prefrontal cortex, specifically the dorsolateral prefrontal cortex (DLPFC), is critically involved in episodic memory (Eichenbaum, 2017) and is the target of most of the noninvasive brain stimulation interventions aimed at improving this function. Crucially, episodic memory impairment is the core hallmark of AD cognitive profile, with trouble putting names to faces representing a distinct clinical manifestation and one of the most disabling symptoms. Accordingly, face–name associative memory tasks, which provide highly sensitive indices of episodic and semantic memory performance, are exploited to capture episodic memory difficulties in AD and can contribute to characterize different stages of disease severity (Parra et al., 2010; Werheid and Clare, 2007). Neuroimaging studies have revealed that in face–name associations, memory requires both highly specialized cortical areas in the occipitotemporal cortex and other brain regions associated with higher cognitive functions, including the DLPFC (D'Esposito et al., 1995; Sperling et al., 2001; Wagner et al., 1998).

Brain connectivity, and more specifically effective connectivity, can be tested by means of the combination of transcranial magnetic stimulation (TMS) with EEG (TMS–EEG). This method allows one to measure cortical excitability and effective connectivity in brain networks by measuring cortical signals evoked by TMS in the target area and their propagation to connected regions (i.e., TMS-evoked potentials [TEPs]) (Bortoletto et al., 2015). TEPs offer an opportunity to probe the causal influence that one region exerts on another because the activation induced by the TMS pulse in the stimulated area spreads to directly or indirectly connected areas. This spread is measured through EEG as amplitude and latency of TEPs generated in remote regions (Bortoletto et al., 2015; Ilmoniemi et al., 1997; Massimini et al., 2005; Morishima et al., 2009). Compared to fMRI-based effective connectivity, TEPs-based effective connectivity has high temporal resolution and low spatial resolution (as determined by EEG properties); its estimation does not require strong a priori assumptions and complex causal models, such as Granger causality. TMS–EEG is an attractive technique because it is noninvasive, painless, and easily accessible (Hohenfeld et al., 2018). Furthermore, being performed in a resting-state condition, TMS–EEG seems particularly suitable for patients with AD, even at

the severe stages of the disease, as it is less demanding for the patient and relatively independent from his/her active collaboration. A few studies have already demonstrated the feasibility of TMS–EEG in AD (Casarotto et al., 2011; Ferreri et al., 2016; Julkunen et al., 2011, 2008) by showing alterations in excitability and connectivity. However, only a very small number of patients have been studied or the target has been the motor cortex, with only marginal relevance in AD clinical manifestations.

The aim of the present study was to determine how prefrontal connectivity alterations are related to AD clinical symptoms and may predict disease severity in overt AD through a cross-sectional design. We explored the relationship between the excitability and effective connectivity of the DLPFC (as derived from TMS–EEG) and cognitive decline (as measured with Mini Mental State Examination [MMSE] and a face–name association memory task) in a sample of patients with overt AD.

2. Material and methods

2.1. Participants

34 right-handed mild to moderate AD patients (age = 77.6, sd = 4.8, range = 64–84; Mini Mental State Examination (MMSE) score = 20.8, sd = 2.3, range = 17–26) were recruited and underwent a clinical and neuropsychological assessment and a TMS–EEG session. Diagnosis of probable AD was done by expert neurologists or geriatricians addressing medical history, clinical examination, neuropsychological testing and laboratory results such as computed tomography, MRI or PET. Inclusion criteria for AD patients were a diagnosis of probable AD according to the criteria of the NINCDS-ADRDA work group (McKhann et al., 1984), MMSE score (Folstein et al., 1975) greater than or equal to 16 and a Clinical Dementia Rating scale score (CDR) from 0.5 to 2. At the time of recruitment, all patients were being treated with cholinesterase inhibitors (donepezil or rivastigmine) or memantine (1 mild and 2 moderate patients) and were on a stable dose for at least 3 months before the beginning of the study. Exclusion criteria were the presence of medical, neurological, or psychiatric disorders that might interfere with the study or the presence of any contraindication for TMS (Rossi et al., 2009). All participants gave their written informed consent before the experiment. All the procedures conformed to the Declaration of Helsinki for research involving human subjects and were approved by the ethics committee of the IRCCS Centro San Giovanni di Dio Fatebenefratelli of Brescia (Italy). Data from 8 participants were excluded from the final sample because of technical problems during TMS–EEG recording. The final sample thus consisted of 26 participants. A subset of 20 patients performed also a face–name association memory task (FNAT). Demographic data from the final sample are reported in Table 1.

2.2. Clinical and neuropsychological assessment

The clinical and neuropsychological assessment, administered by trained neuropsychologists, tested general cognitive abilities (MMSE), memory (Rey Auditory Verbal Learning test; recall of Rey–Osterrieth Complex figure; Story Recall from Rivermead Behavioral Memory test), attentional and executive functions (Trail Making test, part A and B), language (Picture naming task; Battery for Analysis of Aphasic Deficits), and praxis (Rey–Osterrieth Complex figure). All the tests were administered and scored according to standard procedures (Lezak et al., 2012). In addition, functional abilities were evaluated using basic and instrumental activity of daily living (BADL and IADL) scales (Katz, 1983; Lawton and Brody, 1969). The results of the assessments are reported in Table 1.

Table 1
Demographic, clinical, and neuropsychological results

	Total sample (26)	Mild AD (13)	Moderate AD (13)	*p*-value
Demographic and clinical features				
Age (y)	76.5 (4.7)	75.8 (5.2)	77.2 (3.8)	0.44
Gender (males/females)	3/23	2/11	1/12	0.54
Education (y)	7.7 (4.1)	9.1 (5.0)	6.2 (2.1)	0.08
BADL (unspared functions)	0.3 (0.5)	0.3 (0.5)	0.2 (0.6)	0.72
IADL (unspared functions)	3.3 (1.8)	3.2 (1.7)	3.5 (1.7)	0.59
MMSE	20.8 (2.5)	22.8 (1.9)	18.8 (0.9)	<**0.001**
CDR	1.3 (0.5)	0.9 (0.2)	1.7 (0.5)	<**0.001**
Experimental computerized task to assess episodic associative memory				
FNAT, correct responses (%)	28.3 (6.4)	31.6 (5.7)	25.0 (5.2)	**0.02**
Neuropsychological assessment				
Memory				
ROCF recall	0.2 (0.6)	0.2 (0.8)	0.2 (0.4)	0.77
RBM story recall, immediate	1.0 (1.0)	1.4 (1.1)	0.6 (0.6)	0.08
RBM story recall, delayed	0.2 (0.5)	0.4 (0.6)	0.1 (0.3)	0.30
RAVL recall, immediate	18.4 (6.7)	22.7 (6.5)	14.1 (3.2)	**0.002**
RAVL recall, delayed	1.3 (1.5)	2.0 (1.6)	0.6 (1.0)	**0.04**
Praxia				
ROCF copy	16.3 (10.1)	16.4 (9.0)	16.2 (11.0)	0.95
Attentive functions				
TMT A	133.0 (90.6)	91.2 (56.1)	174.8 (98.8)	**0.02**
TMT B	448.3 (117.6)	386.6 (117.0)	510.0 (79.6)	**0.006**
Language				
BADA, oral object naming	66.5 (21.6)	75.6 (21.5)	57.4 (20.3)	**0.04**
BADA, oral action naming	61.3 (21.6)	72.7 (15.1)	49.9 (21.1)	**0.006**
BADA, sentence comprehension	82.9 (10.6)	87.5 (9.7)	78.4 (9.4)	**0.03**

Demographic, clinical, and neuropsychological results of the final sample of patients reported as mean (± standard deviation). Results of the *t*-test or χ^2 test (*p*-value) between mild and moderate AD patients are reported.
Bold *p*-values indicate significant differences between groups.
Key: BADL, Basic Activities of Daily Living; IADL, Instrumental Activities of Daily Living; MMSE, Mini Mental State Examination; CDR, Clinical Dementia Rating scale; FNAT, face—name association task; ROCF, Rey—Osterrieth Complex Figure; RBM, Rivermead Behavioral Memory test; RAVL, Ray Auditory Verbal Learning test; TMT, Trail Making test; BADA, Battery of Analysis of Aphasic Deficits.

2.3. Face—name association memory task

The FNAT is an experimental computerized procedure for assessing episodic associative memory (Cotelli et al., 2014). FNAT included 2 phases: encoding and recognition. The stimuli were displayed on a 15-inch screen 60 cm in front of the patient with the Presentation software (Version 14.9, www.neurobs.com). During the encoding phase, 60 unfamiliar faces paired with a set of 60 unfamiliar first names (30 males, 30 females) were randomly presented. Patients were required to indicate whether the faces belonged to a man or a woman and then were required to encode the face—name associations. In the recognition phase, administered 10 minutes later, previously seen faces were again randomly presented together with 4 proper names (the correct, one novel, and 2 previously presented names). Patients were asked to indicate the correct name for each displayed face. For a detailed description of the task, see Cotelli et al. (Cotelli et al., 2014). FNAT scores are reported in Table 1.

2.4. TMS protocol

TMS was delivered with the Magstim Super Rapid (biphasic) stimulator through a standard 70-mm figure-of-eight coil. Two hundred TMS pulses were delivered over the left DLPFC at random intervals of 2—4 seconds and with stimulus intensity of 110% of the resting motor threshold (rMT). To define rMT, the coil was placed tangentially on the scalp over the left primary motor cortex with the handle pointing backward at about 45° angle from the midsagittal axis of the participant's head. rMT was measured as the lowest stimulus intensity required to elicit a motor-evoked potential of at least 50 μV in the relaxed right first dorsal interosseous for 5 of 10 consecutive trials (Rossini et al., 2015, 1994). The mean rMT was 54.7 percent of the maximal stimulator output (sd = 8.0). To

stimulate the left DLPFC, the coil was positioned tangentially over the scalp at about 45° angle away from the midline, resulting in a posterior—anterior current flow, and targeting the F3 electrode location (according to the International 10—20 System). The coil was held in place by an expert experimenter and monitored throughout the procedure. TMS pulses were delivered during a resting-state condition, with participants comfortably sitting and looking ahead toward a fixation point.

2.5. EEG recording

TMS-compatible EEG equipment (BrainAmp, Brain Products GmbH, Munich, Germany) recorded scalp potentials from 19 (Fp1, Fp2, F7, F3, Fz, F4, F8, T7, C3, Cz, C4, T8, P7, P3, Pz, P4, P8, O1, O2) TMS-compatible sintered Ag/AgCl electrodes (EasyCap, Brain Products). The signal was referenced online with respect to the nose, and the ground electrode was at AFz. Horizontal and vertical eye movements were detected with electrodes placed at the left and right canthi and above and below the right eye, respectively. The impedance between the skin and each electrode was kept below 5 kΩ. A continuous recording mode without the use of any sample-and-hold circuit was adopted. The recorded signal was band-pass-filtered at 0.01—1000 Hz and digitized at a sampling rate of 5000 Hz.

2.6. TMS—EEG analysis

The EEG signals were processed and analyzed offline using EEGLAB (Delorme and Makeig, 2004) and custom scripts on MATLAB (R2016a, The MathWorks, Inc, Natick, Massachusetts). Continuous data were interpolated in the time range from −2 to 10 ms with respect to the TMS pulse and then filtered with a 0.1-Hz high-pass filter. Epochs were created around the TMS pulse, starting from 200 ms before it and ending 500 ms poststimulus. Signal

components corresponding to ocular artifacts (blinks and saccades) were identified and discarded by performing Independent Component Analysis (ICA) with the Infomax ICA algorithm. After ICA, the remaining measurement noise was removed with the SOUND algorithm (Mutanen et al., 2018), which is a Wiener-filtering−based technique designed for noise removal in EEG and magnetoencephalography data. For the purpose of SOUND, the same spherical 3-layer model and the same regularization parameter ($\lambda = 0.01$) as applied in the original work (Mutanen et al., 2018) were used to clean the data. Because TMS−EEG data are likely to contain nonstationary disturbances, the collected data were cleaned with SOUND in 1-ms-long nonoverlapping windows. For estimating the noise covariance matrix at each time window, the 5 samples per trial per each 1-ms window were used. In 5 patients, data were contaminated by TMS-evoked muscle artifacts; then, a method combining signal-space projection and source-informed reconstruction (Mutanen et al., 2016) was applied to project out artifacts during the first 50 ms after the TMS pulse. One muscle-artifact component was removed from each dataset. The muscle-artifact components were identified based on each component's time−frequency behavior and the corresponding signal power as explained in (Mutanen et al., 2016). Following signal-space projection and source-informed reconstruction, data were filtered with a 70-Hz low-pass filter, visually inspected to discard epochs containing residual artifacts, rereferenced to the average of the mastoids and then baseline-corrected using the time interval from −100 to −2 ms.

TEP amplitudes were determined by taking the maximal peak from the electrode exhibiting the highest amplitude in the following time windows: 15−25 ms (positive peak over F3), 25−35 ms (positive peak over Cz), 45−55 ms (positive peak over Cz), and 60−80 ms (positive peak over P4). Later components were not analyzed because components at latencies of 100−200 ms may be related to an auditory-evoked response associated with the sound of the TMS coil discharge (Nikouline et al., 1999) and the sensory response to the TMS on the scalp tissue (Conde et al., 2019).

To characterize how the elicited brain activity spread from the stimulated spot to other areas, we localized each TEP component with sLORETA (sLORETA, Pascual-Marqui, 2002), a distributed source-imaging method. Briefly, sLORETA calculates the standardized neuronal current source density distribution consistent with the scalp topography in the cortical gray matter and the hippocampus of the template of the Montreal Neurological Institute 152 (MNI152) (Fuchs et al., 2002), which comprises 6239 gray-matter voxels at 5-mm spatial resolution. sLORETA estimates the underlying sources under the assumption that the neighboring voxels should have a maximally similar electrical activity; the result is a blurred, widespread solution in which the voxel with maximum current density is identified as the center of the source of the signal. Importantly, a previous systematic comparison study has shown that sLORETA can provide reasonably reliable source-current estimates when the traditional 10−20 system is used (Song et al., 2015).

2.7. Statistical analysis

To investigate how TMS−EEG can predict disease severity, a linear regression was carried out for each TEP component, its amplitude value being the independent variable and the MMSE score the dependent variable. To detect the presence of outliers, Grubbs's test was performed and if significant ($\alpha < 0.05$), outlier values were removed. Outlier calculation identified only a significant value among P70 amplitude values (12.6 μV, $p < 0.05$). To quantify the diagnostic ability of TEP components to discriminate between different stages of disease severity (mild vs. moderate AD), receiver operating characteristic curves were computed for the TEP

components that showed a significant regression equation. The area under the curve index ([AUC]; 0.5<AUC>1, with 1 indicating perfect accuracy) was provided as a measure of diagnostic performance, whereas sensitivity and specificity indices were provided to better evaluate the reliability of TEP components as biomarkers for distinguishing between mild and moderate AD. To do so, patients were classified in accordance with the National Health and Care Excellence guidance (2011) as mild AD if their MMSE score was greater or equal to 21 ($N = 13$; MMSE score $= 22.8 \pm 2.0$; age $= 75.9 \pm 5.6$), and as moderate AD if their MMSE score was equal or less than 20 ($N = 13$; MMSE score $= 18.9 \pm 1.0$; age $= 77.2 \pm 4.0$). In support of the adopted cutoff, MMSE score has been found to discriminate well between all CDR stages with scores of 21−25 and 11−20 corresponding to mild and moderate dementia severity, respectively (Perneczky et al., 2006).

To compare mild and moderate AD patients in demographic, clinical, and neuropsychological data, appropriate statistical tests, that is, t-test for continuous variables and χ^2 for dichotomous variables, have been performed and are reported in Table 1.

Moreover, to study the relationship between each TEP component and episodic memory dysfunction, a linear regression was calculated to predict FNAT performance (dependent variable) from TEP amplitudes (independent variable). Statistical analyses were conducted with IBM SPSS Statistics, Version 20.0 (IBM Corp., Armonk, NY).

3. Results

TMS to the left DLPFC elicited a complex pattern of activity both at the site of stimulation and at other areas. The grand-average waveform (Fig. 1A) shows 6 main components on which sLORETA source localization was performed. The propagation of the evoked activity was traced by means of the scalp distribution of the EEG signals (Fig. 1B) and their cortical source reconstructions (Fig. 1C). The first detected component, peaking approximately at 20 ms (P20, localized in left anterior cingulate), was followed by the activation of the contralateral right superior parietal lobule at 30 ms (P30). The propagation of the signal induced a third component at 50 ms (P50, left superior frontal gyrus), followed by another positive peak at 70 ms (P70, left inferior frontal gyrus). The spatiotemporal evolution of the signal is shown in Fig. 1B−C.

Importantly, the P30 amplitude was predictive of the MMSE score in patients with AD as revealed by the significant linear regression ($F_{(1,21)} = 5.19$, $p = 0.03$, $R^2 = 0.20$) (Fig. 2A). No other significant regression relationship was found. Receiver operating characteristic analysis (Fig. 2B) revealed a good predictive performance of P30 amplitude in discriminating between mild and moderate AD patients (AUC = 0.78). Considering a P30 amplitude value of 3.13 μV as a cutoff score, specificity and sensitivity indexes were 0.63 and 0.92, respectively.

As shown in Fig. 3, a significant regression equation was found also when analyzing the relationship between P30 amplitude and FNAT ($F_{(1,16)} = 5.40$, $p = 0.03$, $R^2 = 0.25$). For the other TEP components, no significant relationship with FNAT was found.

4. Discussion

The aim of the present study was to investigate how prefrontal TMS-evoked activity is associated with disease severity in a sample of mild and moderate AD patients. We found that the amplitude of P30, an early positive EEG response localized by sLORETA algorithm to the right superior parietal lobule, is augmented with more severe cognitive deterioration (lower MMSE score) and that this increase predicts disease severity. In addition, P30 predicted performance in
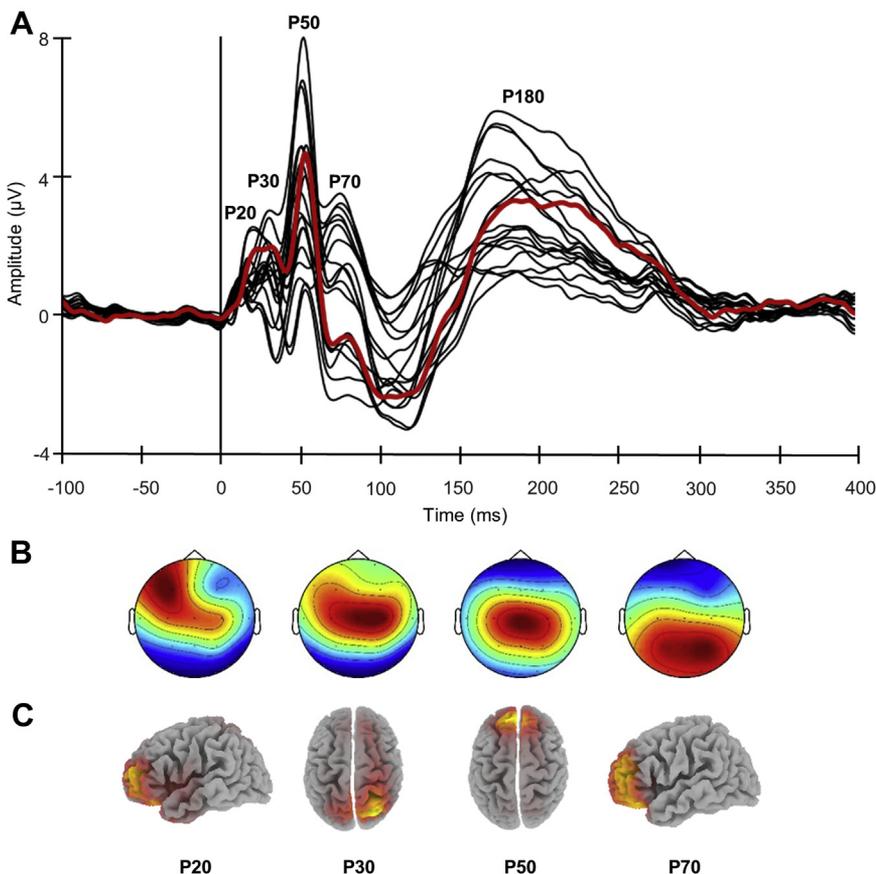
Fig. 1. TMS—EEG results. A) Butterfly plot of the grand-averaged TMS-evoked potentials from all the electrodes showing the main components elicited by left dorsolateral prefrontal cortex (DLPFC) stimulation. The signal from the target site of stimulation (electrode F3) is depicted by the red line; B) Topographic distribution; and C) sLORETA source localization for each TEP component before 100 ms. (For interpretation of the references to color in this figure legend, the reader is referred to the Web version of this article.)

FNAT; a greater amplitude was associated with poorer memory performance.

Despite being elicited by left DLPFC stimulation, P30 did not represent a direct local response of the prefrontal cortex. Source localization results suggested that P30 is generated by the activation of the right superior parietal cortex, possibly due to direct corticocortical signal transmission from the stimulated area. Indeed, the TEP represents the activation of the stimulated area followed by a spatiotemporal propagating pattern of activation (i.e., from the targeted region to other cortical areas that are the later sources of the response) via intrahemispheric and interhemispheric anatomical connections (Bortoletto et al., 2015; Ilmoniemi et al., 1997). Moreover, there is clear evidence of strong connections between prefrontal and parietal areas (Makris et al., 2005). Although TEPs do not demonstrate whether the effect of DLPFC stimulation on posterior parietal cortex is through direct connections or is
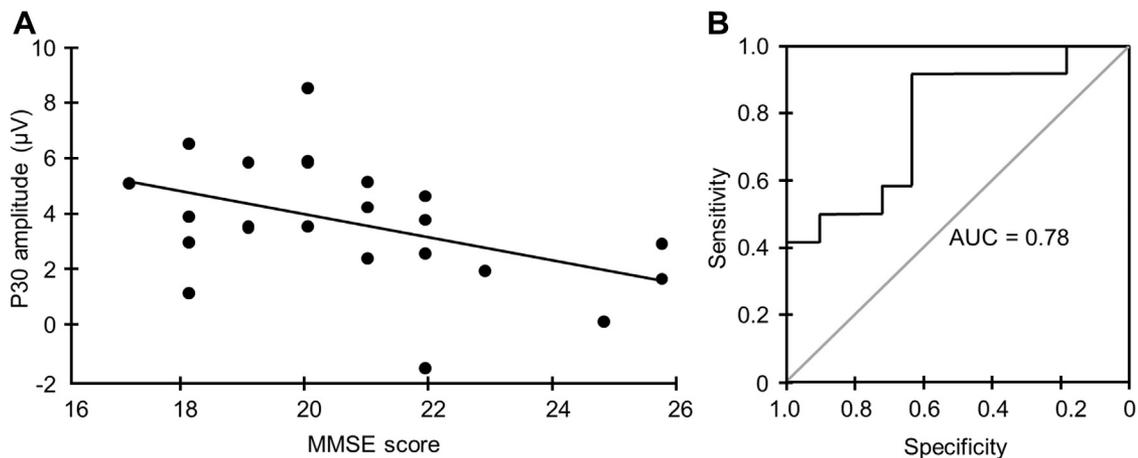

Fig. 2. Relationship between P30 amplitude and MMSE score. A) Scatter plot showing the significant negative correlation between P30 amplitude and Mini Mental State Examination (MMSE) score; B) Receiver operating characteristics curve (ROC) of P30 amplitude discriminating between mild and moderate AD patients. The diagonal line indicates the null hypothesis of AUC = 0.5.
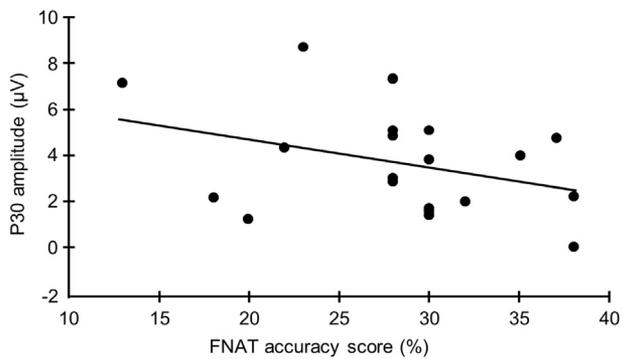
Fig. 3. Relationship between P30 amplitude and FNAT accuracy score. Scatter plot showing the significant negative correlation between P30 amplitude and face–name association memory task (FNAT) accuracy.

mediated by another brain region, they do indicate a causal relation between the stimulation of prefrontal cortex and its effects over other activated areas. Therefore, P30 represents a measure of effective connectivity of long-distance interhemispheric cortical connections between the left DLPFC and the right superior parietal cortex.

The fact that P30 was increased with lower MMSE scores suggests an inverse association between prefrontal-to-parietal connectivity and cognitive decline: as disease severity advances, left DLPFC connectivity becomes stronger. This finding is substantiated by fMRI studies that indicated hyperconnectivity of prefrontal areas in AD (Agosta et al., 2012; Zhang et al., 2016). Investigating functional connectivity between core regions underlying episodic memory performance, Zhang et al. (Zhang et al., 2016) found that the strength of connections between left frontal and right parietal areas increased as a function of disease severity.

It is also interesting to note that the AD-associated alterations of effective connectivity of left DLPFC seem to be selective. P50 and P70, which were localized in other areas of the prefrontal cortex, showed no significant relationship with AD severity. It has been shown that the left DLPFC is part of several networks such as frontoparietal and default-mode networks. It has also been shown that stimulation of DLPFC can activate both of these networks (Opitz et al., 2016). The selective association of P30, with no other effects on the TEP responses within the 100 ms after TMS, may indicate that only specific networks are relevant for the cognitive and memory decline associated with different illness stages. The results of this study do not allow to disentangle which is the network primarily involved in the worsening of AD symptoms but they pave the way for further studies. Cutting-edge TMS–EEG technical improvements will permit to tailor more precisely and individually the stimulation site based on patients' brain scans, thus identifying the target network.

Previous results from TMS–EEG coregistration studies targeting the motor cortex in patients with AD, although partially contrasting, have highlighted a consistent alteration of P30 response. Ferreri et al. (Ferreri et al., 2016) reported local hyperexcitability indexed by an increase in P30 amplitude in mild AD. The authors speculated that higher local activity may reflect plastic reorganization of the sensorimotor system and might serve as a compensatory mechanism able to preserve motor functioning in this sample of patients (Ferreri et al., 2016). Conversely, a previous study showed that P30 amplitude was reduced in early stages of AD, corresponding to a widespread disruption of the sensorimotor system (Julkunen et al., 2008). Moreover, P30 was related with disease severity in mild-stage AD, with decreasing amplitudes for more impaired cognitive functioning (Julkunen et al., 2011).

It has been suggested that gamma-aminobutyric acid (GABA$_A$) postsynaptic receptors are involved in the generation and modulation of P30 (Ferreri et al., 2011). Three classes of receptors (GABA$_A$, GABA$_B$, and GABA$_C$/GABA$_A$-ρ) mediate the inhibitory actions of GABA (the major inhibitory neurotransmitter in the brain); GABA$_A$ regulates most of the fast inhibitory neurotransmission (Rissman and Mobley, 2012). Therefore, P30 might be considered as a signature of corticocortical GABA$_A$ inhibitory circuits, and its increased amplitude might indicate that the moderate stage of AD severity is associated with a boost of inhibitory mechanisms. However, these results were obtained by stimulating the motor cortex, which does not necessarily parallel changes in the prefrontal cortex.

We also explored how prefrontal connectivity alterations at rest reflect memory impairment. P30 was found to predict memory (i.e., FNAT) performance: as P30 amplitude increases, memory impairment worsens. This finding may allow us to understand the functional implication of prefrontal-to-parietal hyperconnectivity, providing suggestions to further disentangle whether such increased recruitment reflects a compensatory or a pathogenic mechanism. The hypothesis of "successful compensation" (Scheller et al., 2014) does not seem to be supported by our results because enhanced prefrontal connectivity is correlated with more severe memory impairment (although a partial compensation may be present). The present finding resonates with the idea put forward by Pievani et al. (Pievani et al., 2014, 2011), who suggested that connectivity enhancement might represent a maladaptive pathogenic mechanism, which, in turn, might reflect damaged excitatory–inhibitory balance between anterior and posterior brain regions. Otherwise, our results might be interpreted in the framework of a failed "attempted compensation" (Scheller et al., 2014), according to which hyperconnectivity is the signature of the ineffective attempt to recruit additional regions to compensate for pathology (Pievani et al., 2014). This does not mean that there cannot be some underlying compensation going on: perhaps, the fast posterior connectivity decline may be compensated by the prefrontal connectivity increase, which may not be sufficient to avoid the functional deficit.

In this sample of patients with AD, P30 amplitude was found to have a good predictive performance (AUC = 0.78) in discriminating between mild and moderate AD, thus endorsing this measure as a potential connectivity marker of disease severity (sensitivity: 92%; specificity: 62%). TMS–EEG has been already successfully applied to develop connectivity-based biomarkers for prediction, diagnosis, or prognosis of various neuropsychiatric conditions (Farzan et al., 2016) such as consciousness disorders (Casali et al., 2013; Ragazzoni et al., 2013) or epilepsy (Kimiskidis, 2016). P30 may thus potentially represent a future connectivity marker able to predict disease severity in overt AD with important implications in AD research as it could help to: 1) monitor the efficacy of clinical interventions (potentially also during TMS therapy) and their ability to modify the course of the disease, 2) identify patients at risk for more severe clinical outcome, and 3) improve understanding of AD pathophysiology (Cummings and Zhong, 2014; Hampel et al., 2010; Hendrickson et al., 2015; Neugroschl and Davis, 2002).

4.1. Limitations and future directions

Although these results appear promising, a few issues need to be considered. First, this study has been performed in a relatively small sample so the results need to be confirmed in larger cohorts. This is particularly important to confirm that TMS–EEG can provide a reliable diagnostic biomarker of AD severity. Second, longitudinal studies assessing long-term changes are needed to take a step toward the development and validation of P30 as

biomarker of AD progression. Indeed, considering the cross-sectional design of the present study, conclusions must be drawn with caution. Third, further studies could attempt to adopt advanced methodological improvements in the acquisition and analysis of TMS–EEG data to obtain more accurate network-based connectivity estimation and thus improve classification accuracy.

5. Conclusions

Despite the growing body of evidence regarding connectivity alterations in AD, only a few studies have investigated how these alterations are associated with clinical symptoms in AD across different severity stages. The present study demonstrated that TMS–EEG can reveal resting-state connectivity alterations related to overt AD which, in turn, are able to predict disease severity. Specifically, we have shown that increased disease severity is associated with a boost in long-distance interhemispheric fronto-parietal signal propagation and connectivity. Our findings allowed also to disentangle the functional implication of prefrontal hyper-connectivity, showing that the additional recruitment possibly represents a maladaptive pathogenic mechanism rather than a true compensatory phenomenon, which might indicate a progressive impairment in the excitatory–inhibitory balance between anterior and posterior brain regions.

Disclosure

Acknowledgements

References

Agosta, F., Pievani, M., Geroldi, C., Copetti, M., Frisoni, G.B., Filippi, M., 2012. Resting state fMRI in Alzheimer's disease: beyond the default mode network. Neurobiol. Aging 33, 1564–1578.

Berendse, H.W., Verbunt, J.P., Scheltens, P., van Dijk, B.W., Jonkman, E.J., 2000. Magnetoencephalographic analysis of cortical activity in Alzheimer's disease: a pilot study. Clin. Neurophysiol. 111, 604–612.

Bortoletto, M., Veniero, D., Thut, G., Miniussi, C., 2015. The contribution of TMS-EEG coregistration in the exploration of the human cortical connectome. Neurosci. Biobehav. Rev. 49, 114–124.

Braak, H., Braak, E., 1991. Neuropathological staging of Alzheimer-related changes. Acta Neuropathol. 82, 239–259.

Brier, M., Thomas, J.B., Snyder, A.Z., Benzinger, T.L., Zhang, D., 2012. Loss of intra- and inter-network resting state functional connections with alzheimer's disease progression. J. Neurosci. 32, 8890–8899.

Buckner, R.L., 2005. Molecular, structural, and functional characterization of alzheimer's disease: evidence for a relationship between default activity, amyloid, and memory. J. Neurosci. 25, 7709–7717.

Buckner, R.L., Andrews-Hanna, J.R., Schacter, D.L., 2008. The brain's default network: anatomy, function, and relevance to disease. Ann. N. Y. Acad. Sci. 1124, 1–38.

Casali, A.G., Gosseries, O., Rosanova, M., Boly, M., Sarasso, S., Casali, K.R., Casarotto, S., Bruno, M.A., Laureys, S., Tononi, G., Massimini, M., 2013. A theoretically based index of consciousness independent of sensory processing and behavior. Sci. Transl. Med. 5, 198ra105.

Casarotto, S., Määttä, S., Herukka, S.K., Pigorini, A., Napolitani, M., Gosseries, O., Niskanen, E., Könönen, M., Mervaala, E., Rosanova, M., Soininen, H., Massimini, M., 2011. Transcranial magnetic stimulation-evoked EEG/cortical potentials in physiological and pathological aging. Neuroreport 22, 592–597.

Conde, V., Tomasevic, L., Akopian, I., Stanek, K., Saturnino, G.B., Thielscher, A., Bergmann, T.O., Siebner, H.R., 2019. The non-transcranial TMS-evoked potential is an inherent source of ambiguity in TMS-EEG studies. Neuroimage 185, 300–312.

Cotelli, M., Manenti, R., Petesi, M., Brambilla, M., Rosini, S., Ferrari, C., Zanetti, O., Miniussi, C., 2014. Anodal tDCS during face-name associations memory training in Alzheimer's patients. Front. Aging Neurosci. 6, 1–9.

Cummings, J., Zhong, K., 2014. Biomarker-driven therapeutic management of alzheimer's disease: establishing the foundations. Clin. Pharmacol. Ther. 95, 67–77.

D'Esposito, M., Detre, J.A., Alsop, D.C., Shin, R.K., Atlas, S., Grossman, M., 1995. The neural basis of the central executive system of working memory. Nature 378, 279–281.

Damoiseaux, J.S., Prater, K.E., Miller, B.L., Greicius, M.D., 2012. Functional connectivity tracks clinical deterioration in Alzheimer's disease. Neurobiol. Aging 33, 828.e19–828.e30.

Delbeuck, X., Van der Linden, M., Collette, F., Linden, M. Van Der, 2003. Alzheimer'Disease as a disconnection syndrome? Neuropsychol. Rev. 13, 79–92.

Delorme, A., Makeig, S., 2004. EEGLAB: an open source toolbox for analysis of single-trial EEG dynamics including independent component analysis. J Neurosci Methods 134, 9–21.

Dubois, B., Feldman, H.H., Jacova, C., DeKosky, S.T., Barberger-Gateau, P., Cummings, J., Delacourte, A., Galasko, D., Gauthier, S., Jicha, G., Meguro, K., O'Brien, J., Pasquier, F., Robert, P., Rossor, M., Salloway, S., Stern, Y., Visser, P.J., Scheltens, P., 2007. Research criteria for the diagnosis of Alzheimer's disease: revising the NINCDS-ADRDA criteria. Lancet Neurol. 6, 734–746.

Eichenbaum, H., 2017. Prefrontal – hippocampal interactions in episodic memory. Nat. Rev. Neurosci. 18, 547–558.

Farzan, F., Vernet, M., Shafi, M.M.D., Rotenberg, A., Daskalakis, Z.J., Pascual-Leone, A., 2016. Characterizing and modulating brain circuitry through transcranial magnetic stimulation combined with electroencephalography. Front. Neural Circuits 10, 73.

Ferreri, F., Pasqualetti, P., Määttä, S., Ponzo, D., Ferrarelli, F., Tononi, G., Mervaala, E., Miniussi, C., Rossini, P.M., 2011. Human brain connectivity during single and paired pulse transcranial magnetic stimulation. Neuroimage 54, 90–102.

Ferreri, F., Vecchio, F., Vollero, L., Guerra, A., Petrichella, S., Ponzo, D., Määtta, S., Mervaala, E., Könönen, M., Ursini, F., Pasqualetti, P., Iannello, G., Rossini, P.M., Di Lazzaro, V., 2016. Sensorimotor cortex excitability and connectivity in Alzheimer's disease: a TMS-EEG Co-registration study. Hum. Brain Mapp. 37, 2083–2096.

Filippi, M., Agosta, F., Scola, E., Canu, E., Magnani, G., Marcone, A., Valsasina, P., Caso, F., Copetti, M., Comi, G., Cappa, S.F., Falini, A., 2013. Functional network connectivity in the behavioral variant of frontotemporal dementia. Cortex 49, 2389–2401.

Folstein, M.F., Folstein, S.E., McHugh, P.R., 1975. "Mini-mental state". A practical method for grading the cognitive state of patients for the clinician. J. Psychiatr. Res. 12, 189–198.

Fuchs, M., Kastner, J., Wagner, M., Hawes, S., Ebersole, J.S., 2002. A standardized boundary element method volume conductor model. Clin. Neurophysiol. 113, 702–712.

Gour, N., Felician, O., Didic, M., Koric, L., Gueriot, C., Chanoine, V., Confort-Gouny, S., Guye, M., Ceccaldi, M., Ranjeva, J.P., 2014. Functional connectivity changes differ in early and late-onset Alzheimer's disease. Hum. Brain Mapp. 35, 2978–2994.

Grady, C.L., Furey, M.L., Pietrini, P., Horwitz, B., Rapoport, S.I., 2001. Altered brain functional connectivity and impaired short-term memory in Alzheimer's disease. Brain 124, 739–756.

Greicius, M.D., Srivastava, G., Reiss, A.L., Menon, V., 2004. Default-mode network activity distinguishes Alzheimer's disease from healthy aging: evidence from functional MRI. Proc. Natl. Acad. Sci. U. S. A. 101, 4637–4642.

Hampel, H., Frank, R., Broich, K., Teipel, S.J., Katz, R.G., Hardy, J., Herholz, K., Bokde, A.L.W., Jessen, F., Hoessler, Y.C., Sanhai, W.R., Zetterberg, H., Woodcock, J., Blennow, K., 2010. Biomarkers for alzheimer's disease: academic, industry and regulatory perspectives. Nat. Rev. Drug Discov. 9, 560–574.

Hendrickson, R.C., Lee, A.Y.H., Song, Q., Liaw, A., Wiener, M., Paweletz, C.P., Seeburger, J.L., Li, J., Meng, F., Deyanova, E.G., Mazur, M.T., Settlage, R.E., Zhao, X., Southwick, K., Du, Y., Holder, D., Sachs, J.R., Laterza, O.F., Dallob, A., Chappell, D.L., Snyder, K., Modur, V., King, E., Joachim, C., Bondarenko, A.Y., Shearman, M., Soper, K.A., Smith, A.D., Potter, W.Z., Koblan, K.S., Sachs, A.B., Yates, N.A., 2015. High resolution discovery proteomics reveals candidate disease progression markers of Alzheimer's disease in human cerebrospinal fluid. PLoS One 10, 1–20.

Hohenfeld, C., Werner, C.J., Reetz, K., 2018. Resting-state connectivity in neurodegenerative disorders: is there potential for an imaging biomarker? Neuroimage Clin. 18, 849–870.

Horwitz, B., Grady, C.L., Schlageter, N.L., Duara, R., Rapoport, S.I., 1987. Intercorrelations of regional cerebral glucose metabolic rates in Alzheimer's disease. Brain Res. 407, 294–306.

Ilmoniemi, R.J., Virtanen, J., Ruohonen, J., Karhu, J., Aronen, H.J., Näätänen, R., Katila, T., 1997. Neuronal responses to magnetic stimulation reveal cortical reactivity and connectivity. Neuroreport 8, 3537–3540.

Julkunen, P., Jauhiainen, A.M., Könönen, M., Pääkkönen, A., Karhu, J., Soininen, H., 2011. Combining transcranial magnetic stimulation and electroencephalography may contribute to assess the severity of Alzheimer's disease. Int. J. Alzheimers Dis. 2011, 654794.

Julkunen, P., Jauhiainen, A.M., Westerén-Punnonen, S., Pirinen, E., Soininen, H., Kononen, M., Paakkonen, A., Maatta, S., Karhu, J., 2008. Navigated TMS

combined with EEG in mild cognitive impairment and Alzheimer's disease: a pilot study. J. Neurosci. Methods 172, 270–276.

Katz, S., 1983. Assessing self-maintenance: activities of daily living, mobility, and instrumental activities of daily living. J. Am. Geriatr. Soc. 31, 721–727.

Kimiskidis, V.K., 2016. Transcranial magnetic stimulation (TMS) coupled with electroencephalography (EEG): biomarker of the future. Rev. Neurol. (Paris). 172, 123–126.

Lawton, M.P., Brody, E.M., 1969. Assessment of older people: self-maintaining and instrumental activities of daily living. Gerontologist 9, 179–186.

Lezak, M.D., Howieson, D.B., Bigler, E.D., Tranel, D., 2012. Neuropsychological Assessment, fifth ed. Oxford University Press, Inc., New York.

Makris, N., Kennedy, D.N., McInerney, S., Sorensen, A.G., Wang, R., Caviness, V.S.J., Pandya, D.N., 2005. Segmentation of subcomponents within the superior longitudinal fascicle in humans: a quantitative, in vivo, DT-MRI study. Cereb. Cortex 15, 854–869.

Massimini, M., Ferrarelli, F., Huber, R., Esser, S.K., Singh, H., Tononi, G., 2005. Breakdown of cortical effective connectivity during sleep. Science 309, 2228–2232.

McKhann, G., Drachman, D., Folstein, M., Katzman, R., Price, D., Stadlan, E.M., 1984. Clinical diagnosis of alzheimer's disease: report of the NINCDS-ADRDA work group under the auspices of department of Health and human services task force on alzheimer's disease. Neurology 34, 939–944.

Morishima, Y., Akaishi, R., Yamada, Y., Okuda, J., Toma, K., Sakai, K., 2009. Task-specific signal transmission from prefrontal cortex in visual selective attention. Nat. Neurosci. 12, 85–91.

Mutanen, T.P., Kukkonen, M., Nieminen, J.O., Stenroos, M., Sarvas, J., Ilmoniemi, R.J., 2016. Recovering TMS-evoked EEG responses masked by muscle artifacts. Neuroimage 139, 157–166.

Mutanen, T.P., Metsomaa, J., Liljander, S., Ilmoniemi, R.J., 2018. Automatic and robust noise suppression in EEG and MEG: the SOUND algorithm. Neuroimage 166, 135–151.

Neugroschl, J., Davis, K.L., 2002. Biological markers in Alzheimer disease. Am. J. Geriatr. Psychiatry 10, 660–677.

Nikouline, V., Ruohonen, J., Ilmoniemi R, J., 1999. The role of the coil click in TMS assessed with simultaneous EEG. Clin Neurophysiol 110, 1325–1328.

Opitz, A., Fox, M.D., Craddock, R.C., Colcombe, S., Milham, M.P., 2016. An integrated framework for targeting functional networks via transcranial magnetic stimulation. Neuroimage 127, 86–96.

Parra, M.A., Abrahams, S., Logie, R.H., Mendez, L.G., Lopera, F., Della Sala, S., 2010. Visual short-term memory binding deficits in familial Alzheimer's disease. Brain 133, 2702–2713.

Pascual-Marqui, R.D., 2002. Standardized low-resolution brain electromagnetic tomography (sLORETA): technical details. Methods Find. Exp. Clin. Pharmacol. 24 (Suppl D), 5–12.

Perneczky, R., Wagenpfeil, S., Komossa, K., Grimmer, T., Diehl, J., Kurz, A., 2006. Mapping scores onto Stages : mini-mental state examination and clinical dementia rating. Am. J. Geriatr. Psychiatry 14, 139–144.

Pievani, M., Agosta, F., Filippi, M., Frisoni, G.B., 2011. Functional brain networks integrity in patients with Alzheimer's disease and mild cognitive impairment. Alzheimers Dement. 7, S218–S219.

Pievani, M., Filippini, N., van den Heuvel, M.P., Cappa, S.F., Frisoni, G.B., 2014. Brain connectivity in neurodegenerative diseases — from phenotype to proteinopathy. Nat. Publ. Gr. 10, 620–633.

Ragazzoni, A., Pirulli, C., Veniero, D., Feurra, M., Cincotta, M., Giovannelli, F., Chiaramonti, R., Lino, M., Rossi, S., Miniussi, C., 2013. Vegetative versus minimally conscious states: a study using TMS-EEG, sensory and event-related potentials. PLoS One 8, e57069.

Rissman, R. a, Mobley, W.C., 2012. Implication for treatment: GABAA receptors in aging, Down syndrome and Alzheimer's disease. J. Neurochem. 117, 613–622.

Rose, S.E., Chen, F., Chalk, J.B., Zelaya, F.O., Strugnell, W.E., Benson, M., Semple, J., Doddrell, D.M., 2000. Loss of connectivity in Alzheimer's disease: an evaluation of white matter tract integrity with colour coded MR diffusion tensor imaging. J. Neurol. Neurosurg. Psychiatry 69, 528–530.

Rossi, S., Hallett, M., Rossini, P.M., Pascual-Leone, A., 2009. Safety, ethical considerations, and application guidelines for the use of transcranial magnetic stimulation in clinical practice and research. Clin. Neurophysiol. 120, 2008–2039.

Rossini, P.M., Barker, A.T., Berardelli, A., Caramia, M.D., Caruso, G., Cracco, R.Q., Dimitrijevic, M.R., Hallett, M., Katayama, Y., Lucking, C.H., Maertens de Noordhout, A.L., Marsden, C.D., Murray, N.M.F., Rothwell, J.C., Swash, M., Tomberg, C., 1994. Non-invasive electrical and magnetic stimulation of the brain, spinal cord and roots: basic principles and procedures for routine clinical application. Report of an IFCN committee. Electroencephalogr. Clin. Neurophysiol. 91, 79–92.

Rossini, P.M., Burke, D., Chen, R., Cohen, L.G., Daskalakis, Z., Di Iorio, R., Di Lazzaro, V., Ferreri, F., Fitzgerald, P.B., George, M.S., Hallett, M., Lefaucheur, J.P., Langguth, B., Matsumoto, H., Miniussi, C., Nitsche, M.A., Pascual-Leone, A., Paulus, W., Rossi, S., Rothwell, J.C., Siebner, H.R., Ugawa, Y., Walsh, V., Ziemann, U., 2015. Non-invasive electrical and magnetic stimulation of the brain, spinal cord, roots and peripheral nerves: basic principles and procedures for routine clinical and research application: an updated report from an I.F.C.N. Committee. Clin. Neurophysiol. 126, 1071–1107.

Scheller, E., Minkova, L., Leitner, M., Kloppel, S., 2014. Attempted and successful compensation in preclinical and early manifest neurodegeneration - a review of task fMRI studies. Front. Psychiatry 5, 1–16.

Song, J., Davey, C., Poulsen, C., Luu, P., Turovets, S., Anderson, E., Li, K., Tucker, D., 2015. EEG source localization: sensor density and head surface coverage. J. Neurosci. Methods 256, 9–21.

Sorg, C., Riedl, V., Mühlau, M., Calhoun, V.D., Eichele, T., Läer, L., Drzezga, A., Förstl, H., Kurz, A., Zimmer, C., Wohlschläger, A.M., 2007. Selective changes of resting-state networks in individuals at risk for Alzheimer's disease. Proc. Natl. Acad. Sci. U. S. A. 104, 18760–18765.

Sperling, R.A., Bates, J.F., Cocchiarella, A.J., Schacter, D.L., Rosen, B.R., Albert, M.S., 2001. Encoding novel face-name associations: a functional MRI study. Hum. Brain Mapp. 14, 129–139.

Sperling, R.A., Dickerson, B.C., Pihlajamaki, M., Vannini, P., LaViolette, P.S., Vitolo, O.V., Hedden, T., Becker, J.A., Rentz, D.M., Selkoe, D.J., Johnson, K.A., 2010. Functional alterations in memory networks in early alzheimer's disease. Neuromolecular Med. 12, 27–43.

Supekar, K., Menon, V., Rubin, D., Musen, M., Greicius, M.D., 2008. Network analysis of intrinsic functional brain connectivity in Alzheimer's disease. PLoS Comput. Biol. 4, e1000100.

Wagner, A.D., Poldrack, R.A., Eldridge, L.L., Desmond, J.E., Glover, G.H., Gabrieli, J.D., 1998. Material-specific lateralization of prefrontal activation during episodic encoding and retrieval. Neuroreport 9, 3711–3717.

Wang, K., Liang, M., Wang, L., Tian, L., Zhang, X., Li, K., Jiang, T., 2007. Altered functional connectivity in early Alzheimer's disease: a resting-state fMRI study. Hum. Brain Mapp. 28, 967–978.

Wang, L., Zang, Y., He, Y., Liang, M., Zhang, X., Tian, L., Wu, T., Jiang, T., Li, K., 2006. Changes in hippocampal connectivity in the early stages of Alzheimer's disease: evidence from resting state fMRI. Neuroimage 31, 496–504.

Werheid, K., Clare, L., 2007. Are faces special in Alzheimer's disease? Cognitive conceptualisation, neural correlates, and diagnostic relevance of impaired memory for faces and names. Cortex 43, 898–906.

Zamboni, G., Wilcock, G.K., Douaud, G., Drazich, E., McCulloch, E., Filippini, N., Tracey, I., Brooks, J.C.W., Smith, S.M., Jenkinson, M., MacKay, C.E., 2013. Resting functional connectivity reveals residual functional activity in Alzheimer's disease. Biol. Psychiatry 74, 375–383.

Zhang, H.Y., Wang, S.J., Liu, B., Ma, Z.L., Yang, M., Zhang, Z.J., Teng, G.J., 2010. Resting brain connectivity: changes during the progress of Alzheimer disease. Radiology 256, 598–606.

Zhang, Y., Simon-Vermot, L., Araque Caballero, M.T., Gesierich, B., Taylor, A.N.W., Duering, M., Dichgans, M., Ewers, M., 2016. Enhanced resting-state functional connectivity between core memory-task activation peaks is associated with memory impairment in MCI. Neurobiol. Aging 45, 43–49.

Zhou, J., Greicius, M.D., Gennatas, E.D., Growdon, M.E., Jang, J.Y., Rabinovici, G.D., Kramer, J.H., Weiner, M., Miller, B.L., Seeley, W.W., 2010. Divergent network connectivity changes in behavioural variant frontotemporal dementia and Alzheimer's disease. Brain 133, 1352–1367.

Web references

National Institute for Health and Clinical Excellence (NICE), 2011. Donepezil, Galantamine, Rivastigmine and Memantine for the Treatment of Alzheimer's Disease: Review of NICE Technology Appraisal Guidance 111. Available at: https://www.nice.org.uk/guidance/ta217. (Accessed 20 June 2018).